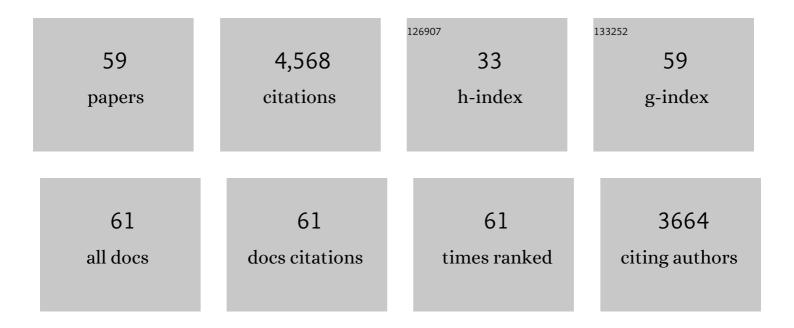
Eric Hellebrand

List of Publications by Year in descending order

Source: https://exaly.com/author-pdf/10215528/publications.pdf Version: 2024-02-01



FDIC HELLERDAND

#	Article	IF	CITATIONS
1	MPI-DING reference glasses for in situ microanalysis: New reference values for element concentrations and isotope ratios. Geochemistry, Geophysics, Geosystems, 2006, 7, n/a-n/a.	2.5	563
2	Coupled major and trace elements as indicators of the extent of melting in mid-ocean-ridge peridotites. Nature, 2001, 410, 677-681.	27.8	528
3	Garnet-field Melting and Late-stage Refertilization in 'Residual' Abyssal Peridotites from the Central Indian Ridge. Journal of Petrology, 2002, 43, 2305-2338.	2.8	321
4	Oceanic core complexes and crustal accretion at slow-spreading ridges. Geology, 2007, 35, 623.	4.4	302
5	Ancient, highly heterogeneous mantle beneath Gakkel ridge, Arctic Ocean. Nature, 2008, 452, 311-316.	27.8	288
6	Diffusion-limited REE uptake by eclogite garnets and its consequences for Lu–Hf and Sm–Nd geochronology. Contributions To Mineralogy and Petrology, 2006, 152, 703-720.	3.1	194
7	Geochemistry of a long in-situ section of intrusive slow-spread oceanic lithosphere: Results from IODP Site U1309 (Atlantis Massif, 30°N Mid-Atlantic-Ridge). Earth and Planetary Science Letters, 2009, 279, 110-122.	4.4	144
8	Abyssal peridotite Hf isotopes identify extreme mantle depletion. Earth and Planetary Science Letters, 2011, 308, 359-368.	4.4	143
9	Clinopyroxene in postshield Haleakala ankaramite: 2. Texture, compositional zoning and supersaturation in the magma. Contributions To Mineralogy and Petrology, 2016, 171, 1.	3.1	115
10	Phosphorus zoning reveals dendritic architecture of olivine. Geology, 2014, 42, 867-870.	4.4	97
11	Trace element distribution between orthopyroxene and clinopyroxene in peridotites from the Gakkel Ridge: a SIMS and NanoSIMS study. Contributions To Mineralogy and Petrology, 2005, 150, 486-504.	3.1	95
12	Significance of large, refractory dunite bodies in the upper mantle of the Bay of Islands Ophiolite. Geochemistry, Geophysics, Geosystems, 2003, 4, .	2.5	92
13	Stacked gabbro units and intervening mantle: A detailed look at a section of IODP Leg 305, Hole U1309D. Geochemistry, Geophysics, Geosystems, 2008, 9, .	2.5	91
14	Magmatic filtering of mantle compositions at mid-ocean-ridge volcanoes. Nature Geoscience, 2009, 2, 321-328.	12.9	91
15	HETEROGENEOUS DISTRIBUTION OF ²⁶ Al AT THE BIRTH OF THE SOLAR SYSTEM. Astrophysical Journal Letters, 2011, 733, L31.	8.3	88
16	Mantle melting beneath Gakkel Ridge (Arctic Ocean): abyssal peridotite spinel compositions. Chemical Geology, 2002, 182, 227-235.	3.3	87
17	Trace element zoning in pyroxenes from ODP Hole 735B gabbros: diffusive exchange or synkinematic crystal fractionation?. Contributions To Mineralogy and Petrology, 2007, 153, 429-442.	3.1	77

Deep melting and sodic metasomatism underneath the highly oblique-spreading Lena Trough (Arctic) Tj ETQq0 0 0 $rg\beta$ T /Overlock 10 Tf 73

ERIC HELLEBRAND

#	Article	IF	CITATIONS
19	Non-chondritic HSE budget in Earth's upper mantle evidenced by abyssal peridotites from Gakkel ridge (Arctic Ocean). Earth and Planetary Science Letters, 2009, 283, 122-132.	4.4	72
20	Heterogeneous distribution of ²⁶ Al at the birth of the solar system: Evidence from refractory grains and inclusions. Meteoritics and Planetary Science, 2012, 47, 1948-1979.	1.6	71
21	Constraints from Os-isotope variations on the origin of Lena Trough abyssal peridotites and implications for the composition and evolution of the depleted upper mantle. Earth and Planetary Science Letters, 2014, 403, 178-187.	4.4	71
22	Diversity of melt conduits in the Izu-Bonin-Mariana forearc mantle: Implications for the earliest stage of arc magmatism. Geology, 2011, 39, 411-414.	4.4	70
23	Clinopyroxene in postshield Haleakala ankaramite: 1. Efficacy of thermobarometry. Contributions To Mineralogy and Petrology, 2016, 171, 1.	3.1	68
24	Phase transition in BCx system under high-pressure and high-temperature: Synthesis of cubic dense BC3 nanostructured phase. Journal of Applied Physics, 2012, 111, .	2.5	67
25	Protracted timescales of lower crustal growth at the fast-spreading East Pacific Rise. Nature Geoscience, 2012, 5, 275-278.	12.9	56
26	Variations in the O-isotope composition of gas during the formation of chondrules from the CR chondrites. Geochimica Et Cosmochimica Acta, 2014, 132, 50-74.	3.9	55
27	Hydrogen incorporation and charge balance in natural zircon. Geochimica Et Cosmochimica Acta, 2014, 141, 472-486.	3.9	54
28	The duration of prograde garnet crystallization in the UHP eclogites at Lago di Cignana, Italy. Earth and Planetary Science Letters, 2009, 287, 402-411.	4.4	51
29	Heterogeneous distribution of 26Al at the birth of the Solar System: Evidence from corundum-bearing refractory inclusions in carbonaceous chondrites. Geochimica Et Cosmochimica Acta, 2013, 110, 190-215.	3.9	42
30	Trace element fractionation during high-grade metamorphism and crustal melting—constraints from ion microprobe data of metapelitic, migmatitic and igneous garnets and implications for Sm–Nd garnet chronology. Lithos, 2006, 87, 193-213.	1.4	40
31	Fluid-present melting of meta-igneous rocks and the generation of leucogranites — Constraints from garnet major- and trace element data, Lu–Hf whole rock–garnet ages and whole rock Nd–Sr–Hf–O isotope data. Lithos, 2009, 111, 220-235.	1.4	37
32	Phosphorus and aluminum zoning in olivine: contrasting behavior of two nominally incompatible trace elements. Contributions To Mineralogy and Petrology, 2019, 174, 1.	3.1	37
33	Conduit- to Localized-scale Degassing during Plinian Eruptions: Insights from Major Element and Volatile (Cl and H2O) Analyses within Vesuvius AD 79 Pumice. Journal of Petrology, 2014, 55, 315-344.	2.8	35
34	Discovery of whitlockite in mantle xenoliths: Inferences for water- and halogen-poor fluids and trace element residence in the terrestrial upper mantle. Earth and Planetary Science Letters, 2006, 244, 201-217.	4.4	34
35	Hydrogen bond symmetrization and equation of state of phase D. Journal of Geophysical Research, 2011, 116, .	3.3	29
36	Geochemical Composition of K-rich Lavas from the Lena Trough (Arctic Ocean). Journal of Petrology, 2011, 52, 1185-1206.	2.8	24

ERIC HELLEBRAND

#	Article	IF	CITATIONS
37	Textural, geochronological and chemical constraints from polygenetic titanite and monogenetic apatite from a mid-crustal shear zone: An integrated EPMA, SIMS, and TIMS study. Chemical Geology, 2007, 241, 88-107.	3.3	22
38	An alternative model for silica enrichment in the Kaapvaal subcontinental lithospheric mantle. Geochimica Et Cosmochimica Acta, 2009, 73, 6894-6917.	3.9	21
39	High-pressure Reactive Melt Stagnation Recorded in Abyssal Pyroxenites from the Ultraslow-spreading Lena Trough, Arctic Ocean. Journal of Petrology, 2014, 55, 427-458.	2.8	21
40	Tectonic, diapiric and sedimentary chaotic rocks of the Rakhine coast, western Myanmar. Gondwana Research, 2019, 74, 126-143.	6.0	20
41	Oxygen isotope and chemical compositions of magnetite and olivine in the anomalous CK3 Watson 002 and ungrouped Asukaâ€881595 carbonaceous chondrites: Effects of parent body metamorphism. Meteoritics and Planetary Science, 2014, 49, 1456-1474.	1.6	19
42	Formation of the high pressure graphite and BC ₈ phases in a cold compression experiment by Raman scattering. Journal of Raman Spectroscopy, 2013, 44, 1596-1602.	2.5	18
43	Magmatic and hydrothermal activity in Lena Trough, Arctic Ocean. Eos, 2001, 82, 193-193.	0.1	17
44	Elastic characterization of platinum/rhodium alloy at high temperature by combined laser heating and laser ultrasonic techniques. Ultrasonics, 2014, 54, 963-966.	3.9	17
45	Oblique nonvolcanic seafloor spreading in Lena Trough, Arctic Ocean. Geochemistry, Geophysics, Geosystems, 2011, 12, n/a-n/a.	2.5	15
46	Cryogenic Minerals in Hawaiian Lava Tubes: A Geochemical and Microbiological Exploration. Geomicrobiology Journal, 2018, 35, 227-241.	2.0	15
47	The P–T–t paths of high-grade gneisses, Kaoko Belt, Namibia: Constraints from mineral data, U–Pb allanite and monazite and Sm–Nd/Lu–Hf garnet ages and garnet ion probe data. Gondwana Research, 2014, 25, 775-796.	6.0	14
48	Olivine–wadsleyite–pyroxene topotaxy: Evidence for coherent nucleation and diffusion-controlled growth at the 410-km discontinuity. Physics of the Earth and Planetary Interiors, 2012, 200-201, 85-91.	1.9	13
49	Crystallochemistry and origin of pyroxenes in komatiites. Contributions To Mineralogy and Petrology, 2009, 158, 599-617.	3.1	12
50	Potential for Tufa Precipitation from Crushed Concrete Containing Coarse Basaltic and Fine Coralline Sand Aggregates. Environmental and Engineering Geoscience, 2011, 17, 53-66.	0.9	10
51	Chemical heterogeneities reveal early rapid cooling of Apollo Troctolite 76535. Nature Communications, 2021, 12, 7054.	12.8	8
52	Incipient melt segregation as preserved in subaqueous pyroclasts. Geology, 2012, 40, 355-358.	4.4	6
53	Extensive Magmatic Heating of the Lithosphere Beneath the Hawaiian Islands Inferred From Salt Lake Crater Mantle Xenoliths. Geochemistry, Geophysics, Geosystems, 2020, 21, e2020GC009359.	2.5	4
54	Intracrystalline melt migration in deformed olivine revealed by trace element compositions and polyphase solid inclusions. European Journal of Mineralogy, 2021, 33, 463-477.	1.3	4

#	Article	IF	CITATIONS
55	Celestine discovered in Hawaiian basalts. American Mineralogist, 2020, 105, 52-57.	1.9	2
56	Geochemistry of ultramafic and mafic rocks from the northern Central Asian Orogenic Belt (Tuva,) Tj ETQq0 0 0 r intra-oceanic subduction. Precambrian Research, 2021, 356, 106061.	gBT /Over 2.7	lock 10 Tf 50 2
57	A Study in Blue: Secondary Copperâ€Rich Minerals and Their Associated Bacterial Diversity in Icelandic Lava Tubes. Earth and Space Science, 2022, 9, .	2.6	2
58	Volcanic glass at Kualoa, Oâ€~ahu, Hawaiian Islands: Paired technological and geochemical sourcing analyses of an expedient tool industry. Journal of Archaeological Science: Reports, 2020, 30, 102117.	0.5	1
59	Peridotite. , 2014, , 1-2.		0